



HAL
open science

Estimation of Soil Moisture Content on Spectral Reflectance of Bare Soils in the 0.4 -2.5 μm Domain

S. Fabre, A. Leassignoux, X. Briottet

► **To cite this version:**

S. Fabre, A. Leassignoux, X. Briottet. Estimation of Soil Moisture Content on Spectral Reflectance of Bare Soils in the 0.4 -2.5 μm Domain. *Sensors*, 2014, pp.1-18. 10.3390/s150203262 . hal-01096413

HAL Id: hal-01096413

<https://hal.science/hal-01096413>

Submitted on 17 Dec 2014

HAL is a multi-disciplinary open access archive for the deposit and dissemination of scientific research documents, whether they are published or not. The documents may come from teaching and research institutions in France or abroad, or from public or private research centers.

L'archive ouverte pluridisciplinaire **HAL**, est destinée au dépôt et à la diffusion de documents scientifiques de niveau recherche, publiés ou non, émanant des établissements d'enseignement et de recherche français ou étrangers, des laboratoires publics ou privés.

Article

Estimation of Soil Moisture Content on Spectral Reflectance of Bare Soils in the 0.4 -2.5 μm Domain

S. Fabre ^{1,*}, A. Lesaignoux ² and X. Briottet ¹

¹ Onera, BP740252 avenue Edouard Belin FR-31055 TOULOUSE CEDEX 4;
E-Mails: sophie.fabre@onera.fr, xavier.briottet@onera.fr;

² DomPas Internet Inc., 6719 rue Vézina Québec G3E 2J4 Canada ;
E-Mail: audrey@dompasinternet.ca,

* Author to whom correspondence should be addressed; E-Mail: sophie.fabre@onera.fr;
Tel.: +33 5 62 25 28 59.; Fax: +33 5 62 25 25 88

Received: / Accepted: / Published:

Abstract: The purpose of this paper is to define a method of soil moisture content estimation for bare soils based on their spectral signatures in the reflective domain. In a first time, this work consists in defining the most efficient and robust methods existing in the literature. Two spectral indexes are then retained. In a second time, new methods are proposed to overcome their limitations. Owing to correlation matrix tool, two other spectral indexes are defined by tacking into account atmosphere impact. Moreover, two global methods are defined. The first one is based on the Gaussian model found in the literature and the second one uses an existing empirical soil model. All these methods are compared on a reference database composed of the spectral signatures and the related soil moisture contents measured in laboratory for many soil samples. Finally, a realistic case is simulated in order to analyse the impact of a given hyperspectral instrument specifications and the influence of the atmospheric water vapour content on all the methods.

Keywords: Soil moisture content, bare soil, spectral reflectance, spectral indexes, soil model.

1 Introduction

The knowledge of surface soil moisture is crucial for many applications like trafficability after flood, soil – atmosphere exchanges or plant good health. Remote sensing technics (optical to radar) have several advantages in comparison with others in situ methods (gravimetric, electromagnetic, thermal...) for monitoring Soil Moisture Content (SMC) [1], as they provide better temporal and spatial coverage [2]. One of the most challenging remote sensing techniques to estimate the SMC is the hyperspectral imagery [3]. Indeed, near future missions like PRISMA (Hyperspectral Precursor of the Application Mission) [4] and EnMAP (Environmental Mapping and Analysis Program) [5] will be launched in 2015 and 2017, respectively. These two missions will cover the reflective domain from 0.4 μm to 2.5 μm with a 10 nm spectral resolution. Such technical and instrumental characteristics open the way to retrieve SMC as proposed by [6] and [7].

Angström [8] demonstrated through lab measurements that soil moisture content had an impact on the behavior of soil spectral reflectances in the solar domain. This work exhibited a decrease of the reflectance level as SMC increased due to a darkening of the soil surface. Later, other lab acquisitions over bare soils [9] [10] confirmed this behavior which has, then, been used to develop SMC approaches from spectral reflectance.

The investigation to explore the possibility of estimating soil moisture content from multispectral or hyperspectral remote sensing data, was penalized by the lack of specific database. Liu *et al.* [10] measured the spectral reflectances of ten soil samples and characterized the SMC during a drying process. These measurements have been completed by the database described in [17] including the spectral reflectances of thirty natural soil samples in [0.4 – 2.5 μm] depending on the SMC and measured in laboratory. This database was used to analyze the relationship between the soil moisture content and the reflectance spectra. The laboratory measurements was limited to few SMC levels (five or six) according to experimental constraints (drying time for example). In order to go beyond this limitation, a semi-empirical soil model useful to simulate bare soil spectral reflectances for SMC levels not reached by experimentation was then proposed in [17] and compared to other models in the literature. These works showed that the database development is a necessary stage to analyze the impact of SMC variation on soil spectral reflectances, to model this spectral behavior according to SMC and then to specify robust SMC assessment methods based on spectral signature in the [0.4 – 2.5 μm] domain.

At present time, in solar domain, three main approaches of SMC assessment can be distinguished: combination of spectral bands [6] [11] [12], exponential or gaussian spectral model [7] [13], and geostatistical methods [14] [15] [16]. The combination of spectral bands leads to the development of analytical methods and spectral indexes. Liu *et al.* [11] tested the first type of approaches using eighteen bare soils samples at different moisture contents characterized in laboratory. They used several analytical methods: a relative approach, which normalized spectral reflectance of wet soil by spectrum of dry soil, a derivative approach, which applied finite difference method on spectra, and an approach by difference, which computed a waveband difference. Their results showed that SMC estimation was more efficient using the relative method in the SWIR (Short Wavelength InfraRed) domain [1.4 – 2.5 μm]. Concerning the use of spectral indexes for estimating soil moisture of bare soils, the best results were obtained with WISOIL [2], SASI (Shortwave Angle Slope Index) [12] and

NSMI (Normalized Soil Moisture Index) [6]. Purpose of these indexes has been validated by reflectance measurements at different SMC over different bare soils. Lobell *et al.* [13] have developed a spectral exponential model that was applied on four bare soil spectra measured in laboratory. Their results confirmed the strong potential of the SWIR domain for SMC estimation. Another model, the SMGM (Soil Moisture Gaussian Model) [7], applied on spectral reflectances in the SWIR at different moisture contents, showed the possibility to derive a good indicator of SMC from the area under the reflectance spectra in [1.8 – 2.8 μm]. Geostatistical methods [14] [15] [16] pointed out the influence of topography in soil moisture estimation from in situ measurements.

The objective of this article is then to define new methods of SMC estimation based on the spectral signature of bare soils. Two approaches are then investigated to reach this objective : the local methods like spectral indexes and the global methods using the general shape of the spectral signature. The proposed methods are compared to the most efficient methods in the literature.

This paper is organized as follows: Section 2 presents the used database and soil spectral model. Section 3 describes the methods of the SMC estimation. Section 3 presents the performances of SMC assessment methods applied to laboratory measurements and simulated data. Finally, conclusions follow in section 4.

2 Description of the Used Reference Data and Soil Spectral Model

2.1 Reference Database

The choice of the reference database in the literature is made in relation to the number of samples, the disparity of their contrasts and the number of SMC levels. The database developed by Lesaignoux *et al.* described in details in [17] is then used. About thirty natural soil samples, covering different ranges of composition (clay, limestone, sandy) and coloration, were collected over eight locations in France (from South-West to South-East of France) (Table 1).

Table 1. Information of bare soil samples area name defining as [France Department ID][Nearby Town], number of collected samples, area geographic location, Munsell color code (Y: yellow; YR: yellow red). Extracted from [17].

Area name	Number	Geographic location		Munsell color code [18]		
		Latitude	Longitude	Hue	Value	Chroma
11Belvis	1	42°51'02''N	02°04'32''E	2,5Y	6	6
11Malves	1	43°15'08''N	02°26'26''E	2,5Y	7	4
12Vabres	1	43°41'35''N	02°25'35''E	2,5YR	4	4
13Crau	2	43°8'59''N	06°04'27''E	10YR	4	6
				10YR	5	4
24Coulouniex	1	45°11'11''N	00°42'00''E	2,5Y	4	2
30Camargue	19	43°40'37''N	04°37'43''E	2,5Y	5	2
				2,5Y	6	2
30Pujaut	1	44°00'17''N	04°46'29''E	2,5Y	8	1
31Fauga	2	43°23'47''N	01°17'39''E	2,5Y	4	3
31Lauraguais	2	43°23'59''N	01°43'05''E	2,5Y	5	4
				2,5Y	5	3
81Lautrec	1	43°42'22''N	02°08'20''E	2,5Y	3	3
81StJulien	1	43°59'22''N	02°20'45''E	5Y	8	1
84Avignon	1	43°56'55''N	04°48'30''E	2,5Y	7	2

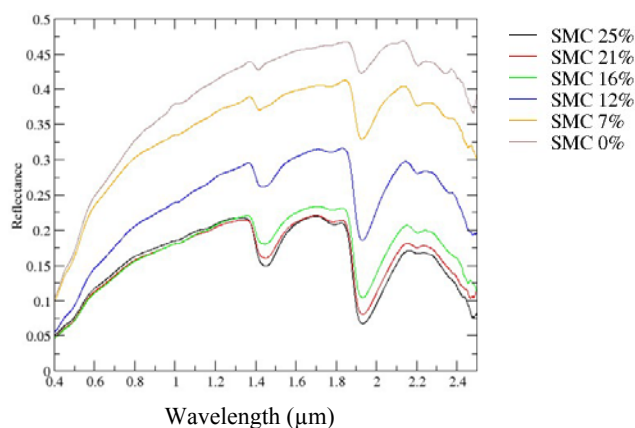
Then, the spectral reflectance measurements of these bare soils were performed in laboratory for different SMC (five or six levels). The laboratory facility and protocol measurements are described in [17]. The impact of soil moisture on spectral reflectances and the soil classification according to spectral behaviour are only remained in the next paragraphs.

2.2 SMC Impact on Soil Spectral Reflectances

The increasing of SMC value leads to [10] [11] [17] (Figure 1):

- A decrease of the global reflectance level on the spectral domain [0.4-2.5 μm] until a SMC threshold value where the inverse relationship is observed;
- A reduction of the mineral absorption bands;
- A decrease of the amplitude and the width of the water absorption bands specially at 1.4 μm and 1.9 μm .

Figure 1. Spectral signature according to SMC for a soil sample extracted from database defined in [17].



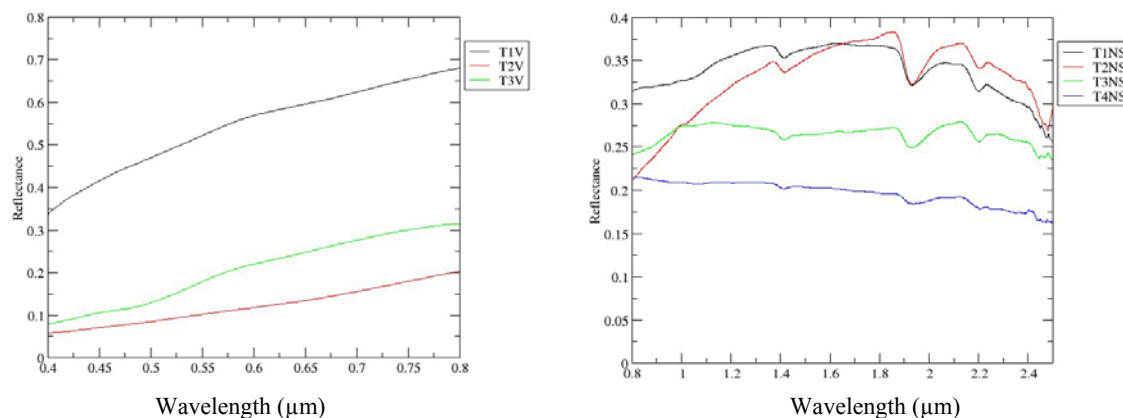
In [17], the reflectance measurements of dry samples were compared to saturated sample ones. Spectral behaviour were analysed according to the following spectral intervals : Visible (VIS) domain [0.4 – 0.8 μm] and Near and Shortwave InfraRed (NSWIR) domain [0.8 – 2.5 μm].

Globally, the reflectance difference between dry and saturated samples was less than 0.13 (± 0.04) in VIS and 0.3 (± 0.08) in NSWIR (for the entire sample data set). The efficiency of the NSWIR domain to SMC assessment in comparison to the VIS domain has been demonstrated. In NSWIR, the absorption peak depth of hydroxyl (OH^-), at 1.4 μm and 1.9 μm increases and gets broader with SMC. A loss of absorption peak of the hydroxyl (OH^-) at 2.2 μm (Figure 1) is noted, which this ion is probably not linked to water but to other minerals. Indeed, some minerals are composed of hydroxyl ion, and an enhancement of SMC involves a decrease of minerals absorption depth [6] [17].

2.3 *A priori classification of spectral signature of dry soil samples*

In [17], the spectral reflectance database related to SMC, achieved by the measurements described in the section 2.1, was kept to group together soils with the same spectral behavior, called *a priori* soil class. The Figure 2 illustrates the observed spectral behaviours of dry samples in the VIS and NSWIR spectral domains.

Figure 2. Spectral behaviours of dry soil samples (left : VIS [0.4 – 0.8 μm], right : NSWIR [0.8 – 2.5 μm]).



According to [17], the soil samples are then grouped together in seven *a priori* spectral classes defined by Table 2.

Table 2. The *a priori* spectral classification of soil samples.

<i>A priori</i> soil spectral class	Spectral behaviour identification (Figure 2)	Soil sample number
Class 1	T3V – T1NS	5
Class 2	T3V – T3NS	1
Class 3	T3V – T2NS	19
Class 4	T2V – T2NS	3
Class 5	T1V – T1NS	1
Class 6	T3V – T4NS	2
Class 7	T1V – T3NS	1

2.4 Semi-empirical Soil Model

The empirical soil model is chosen among those in literature according to its performance and robustness. The integration of SMC in the model is necessary for our objective. The semi-empirical soil model detailed in [17] is then retained. It links the spectral reflectance with the SMC for a given *a priori* soil class. This mathematical model was defined according to the reference database described in section 2.1.

The proposed mathematical model is then defined by the following equation [17] :

$$\rho_{SMC_g}^l(\lambda) = a_l(\lambda) \cdot SMC_g^2 + b_l(\lambda) \cdot SMC_g + c_l(\lambda) \quad (1)$$

where l designs the soil spectral class, a , b and c are the spectral coefficients of the polynomial function in the solar domain.

3 Description of the Methods to Estimate the Soil Moisture Content

Two categories of methods can be distinguished: the local methods based on the combination of particular spectral bands and the global methods using the shape of the spectral signature over a spectral range.

3.1 Local Methods : Spectral Indexes

3.1.1 Indexes in the Literature

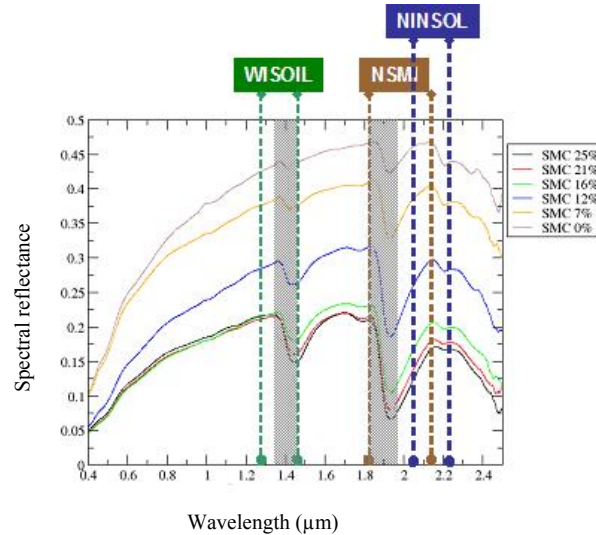
The most robust indexes in the literature are chosen : Normalized Soil Moisture Index (NSMI) [6] and WISOIL [2]. They are described in the Table 3.

Table 3. Existing spectral indexes suitable for SMC assessment (ρ reflectance).

Spectral index	Used spectral bands	Formulation
NSMI	1,8 μm ; 2,119 μm	$\frac{\rho_{1,8} - \rho_{2,119}}{\rho_{1,8} + \rho_{2,119}}$
WISOIL	1,3 μm ; 1,45 μm	$\frac{\rho_{1,45}}{\rho_{1,3}}$

One of their drawbacks is due to the use of spectral bands close to the spectral absorption bands of atmospheric water vapour (centred on the 1.4 μm and 1.9 μm wavelengths) (Figure 3).

Figure 3. Spectral wavelengths of interest for local methods. The gray lines represent the atmospheric water vapour absorption bands.



3.1.2 New Indexes

We propose in this work to define a new index overcoming this limitation. To this end, the procedure proposed by Haubrock *et al.* and based on the correlation matrix is achieved [6]. In literature only linear correlations are used and we propose to complete the linear correlation coefficient (Pearson) with the non-linear correlation coefficient (Spearman).

The correlation is then computed for the two quantities $X_{norm}(\lambda_i, \lambda_j)$ (normalized ratio) and $X_{slope}(\lambda_i, \lambda_j)$ (slope) defined by the following equations:

$$X_{norm}(\lambda_i, \lambda_j) = \frac{\rho(\lambda_i) - \rho(\lambda_j)}{\rho(\lambda_i) + \rho(\lambda_j)} \quad (2)$$

$$X_{slope}(\lambda_i, \lambda_j) = \frac{\rho(\lambda_i) - \rho(\lambda_j)}{\lambda_i - \lambda_j} \quad (3)$$

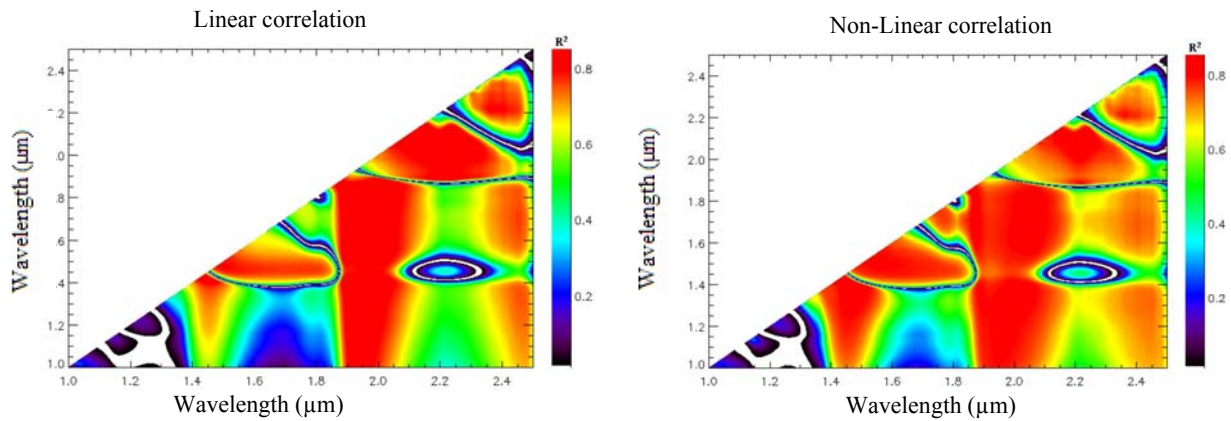
where $\rho(\lambda_i)$ and $\rho(\lambda_j)$ respectively represents the reflectance values at the wavelengths λ_i and λ_j belonging to the reflective domain [0.4 – 2.5 μm].

According to laboratory measurements described in 2.1 and the analysis of the SMC impact on spectral signature, the wavelength couples (λ_i, λ_j) which are very sensitive to SMC are located in the spectral range [1 – 2.5 μm] for the $X_{norm}(\lambda_i, \lambda_j)$ quantity. The results of the correlation matrix for this quantity applied on the reference database are shown on Figure 4. The highest R^2 correlation coefficients are around 80% for wavelengths located in the [2–2.4 μm] range. The wavelength couples that lead to the higher correlation coefficient between the SMC and the quantity $X_{norm}(\lambda_i, \lambda_j)$ are then the followings :

- 2.076 – 2.,228 μm for $X_{norm}(\lambda_i, \lambda_j)$: $R^2 = 87\%$ - linear correlation
- 2.,122 – 2.23 μm for $X_{norm}(\lambda_i, \lambda_j)$: $R^2 = 87\%$ - non linear correlation.

The impact of atmospheric water vapour absorption bands has been taken into account to choose these wavelengths (Figure 3).

Figure 4. Linear (left) and non-linear (right) correlation matrix for $X_{norm}(\lambda_i, \lambda_j)$ computed with the reference database in the [1-2.5 μm] domain.



These results lead to the following spectral indexes:

- NINSOL (Normalized Index of Nswir domain for Smc estimatiOn from Linear correlation)

$$NINSOL = \frac{\rho_{2.076} - \rho_{2.23}}{\rho_{2.076} + \rho_{2.23}} \quad (4)$$

- NINSON (Normalized Index of Nswir domain for Smc estimatiOn from Non linear correlation)

$$NINSON = \frac{\rho_{2.122} - \rho_{2.23}}{\rho_{2.122} + \rho_{2.23}} \quad (5)$$

3.2 Global Methods

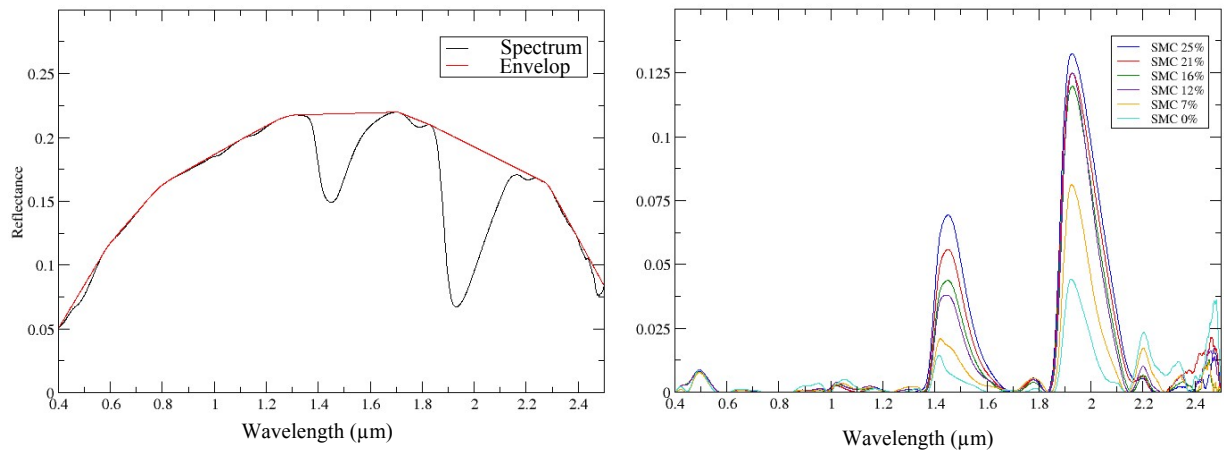
Two global methods are considered: the convex envelope model based on SMGM [19] and the inversion of the soil empirical reflectance model described in 2.4.

3.2.1 Convex Envelope Model

Whiting *et al.* [19] use the convex envelope to adjust an inverse Gaussian to the spectrum shape in the spectral interval [1.8- 2.8 μm]. One drawback of this method is that it is not much more applicable for SMC lower than a threshold value. We propose an alternative to overcome this limitation by extending the inverse Gaussian to the general spectrum shape of the entire solar spectrum [0.4 – 2.5

μm] (Figure 5, left). The area under the curve achieved by subtracting the convex envelope and the spectrum is the criteria linked to SMC (Figure 5, right).

Figure 5. Illustration of the convex envelope method applied on a measured spectral signature (left) and the difference between convex envelope and spectrum according to SMC (right).



The area under the convex envelope increases with SMC (Figure 5, left). The relation between the SMC and this area is then modelled by a linear regression.

3.2.2 Inverse Soil Empirical Reflectance Model

The semi-empirical soil reflectance model (see paragraph 2.4) is inverted in order to provide, for a given *a priori* soil class and the related spectral signature, the corresponding SMC. For each soil spectra, the inverse model is then assessing SMC by using the equation of the direct model (Equation (1)).

The inversion method is to perform, for each retained *a priori* soil spectral class, N spectral signature modelings corresponding to N SMC values. N is fixed by the number of measured SMC levels for the considered soil class. For each wavelength, the input reflectance value is compared to the N simulated reflectances. The most relevant SMC value is the SMC which minimizes the quadratic error defined by the following equation:

$$E = \sum_{i=0}^q \left(\rho_{input}(i) - (a_l(i) \cdot SMC_g^2 + b(i) \cdot SMC_g + c(i)) \right)^2 \quad (6)$$

Where i is the wavelength, ρ_{input} is the spectral reflectance for which the associated SMC value is searched and q is the wavelength number.

In the next, the Inverse Soil Empirical Reflectance model is called ISER model.

4 Results and Discussion

The methods of SMC assessment described in the paragraph 3 are applied on the reference spectral signatures defined in the paragraph 2.1 in order to assess and compare their performances.

The performances are measured owing to two criteria : the correlation coefficient R^2 and the Root Mean Square Error (RMSE).

4.1 Comparison of the SMC Assessment Methods Global

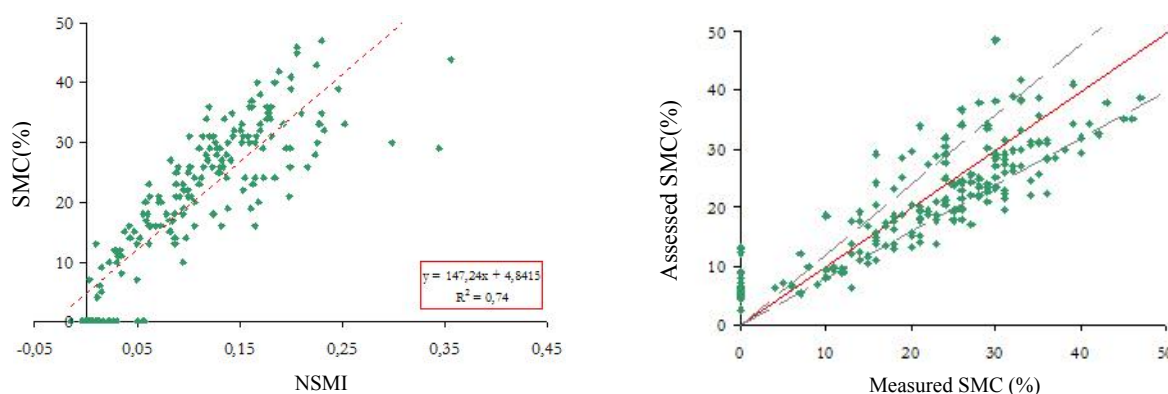
4.1.1 Local Methods

The principle of this validation stage is illustrated by the Figure 6 and breaks down as follows:

- The index is computed for all the measured spectral signatures described in the paragraph 2.1,
- The SMC is represented according to computed index in order to deduce linear (or non linear) regression between SMC and index (Figure 6, left - regression represented by the red dotted line) and to compute the corresponding R^2 value,
- The SMC is then assessed owing to the linear (or non linear) relation and represented according to measured SMC introduced in the paragraph 2.1 (Figure 6, right).

For the indexes suggested by the literature, 52% of the SMC values obtained with NSMI have an relative error greater than 20 % (24 % for WISOIL). Moreover, these two criteria undervalue the SMC.

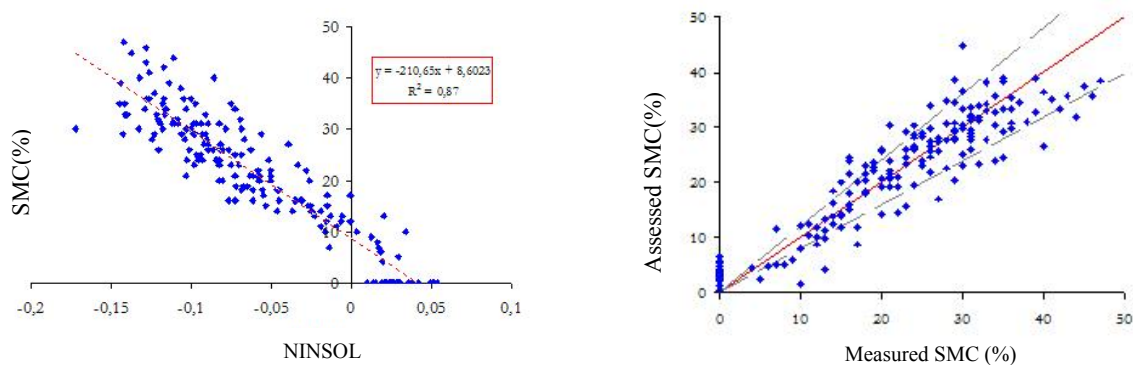
Figure 6. Variation of the NSMI according to SMC (left) and representation of assessed SMC with NSMI according to measured SMC (right). The dashed black lines represent the boundaries of a relative error of 20%.



For the proposed indexes described in the paragraph 3.1.2 (Equations (4) and (5)), the R^2 values of NINSOL and NINSON are respectively of 87% and 85 %. These values are better than those obtained

with WISOIL and NSMI. The results for NINSON are illustrated by the Figure 7. For the two proposed indexes 70 % of the estimated SMC values are characterized by an error lesser than 20 %.

Figure 7. Variation of the NINSOL according to SMC (left) and representation of assessed SMC with NINSOL according to measured SMC (right). The dashed black lines represent the boundaries of a relative error of 20%.



4.1.2 Global Methods

The same validation process is applied to convex envelope model based on SMGM and the ISER model (§ 3.2).

For the convex envelop model, the correlation coefficient R^2 between the SMC and the area under the curve is equal to 80 % with a corresponding RMS error of 5.6 %.

The comparison between the assessed SMC by the ISER model and the measured SMC is illustrated for each *a priori* soil spectral class in the Table 4. The RMSE ranges between 2 and 4 % according to the *a priori* soil class.

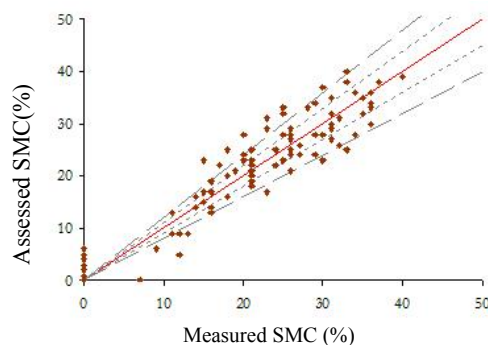
Table 4. RMSE values obtained with the inverse model for each *a priori* soil class.

Soil spectral class	RMSE(%)
Class 1	4.1
Class 2	2.2
Class 3	4.0
Class 4	3.6
Class 5	1.9
Class 6	3.7
Class 7	2.1

The soil spectral classes composed by an unique soil (class 2, class 5 and class 7) have RMSE values lower than 3 % and the corresponding relative error is lower than 10%.

The soil class 3, which including the largest number of samples, is mainly characterized by an error on the SMC estimation lower than 20 % (Figure 8).

Figure 8. Representation of assessed SMC with the inverse model according to measured SMC for the a given *a priori* soil class. The dashed black lines represent the boundaries of a relative error of 20%.



4.1.3 Synthesis

A conclusion on the performances of the different methods is given in Table 5.

The performances of the area under the convex envelop are equivalent to WISOIL and NSMI performances. The capacities of the inverse soil spectral model to retrieve SMC are closely approximates that of the NINSOL and NINSON. All the global and local methods, except for inverse soil spectral model, can be applied whatever the soil type. The inverse model needs the soil spectral class as input.

Table 5. Synthesis of the methods and their performances.

Method	Type	Reference	Performance (RMSE)
NSMI	Local	[6]	6 %
WISOIL	Local	[2]	6 %
NINSOL	Local	§ 3.1.2	4.4 %
NINSON	Local	§ 3.1.2	4.8 %
Envelop convex model	Global	§ 3.2.1	6 %
Inverse soil spectral model	Global	§ 3.2.2	3.8 %

4.2 Analysis of the Atmosphere Impact on the SMC Assessment Methods : Application to a Realistic Simulation Case

In order to test the applicability of the local and global methods to outdoor measurements and to evaluate their robustness, the SMC methods are applied on spectral radiances simulated at the top of the atmosphere for specific spectral bands corresponding to existing hyperspectral system. This requires the definition of a direct and an inverse simulators. The direct simulator is based on the radiative transfer code MODTRAN4 (MODerate resolution atmospheric TRANsmission ; [20], [21])

and allows to model spectral radiance at sensor level owing to spectral reflectance at ground level (in our case laboratory measurements). The inverse simulator is based on the atmospheric correction code Cochise (COde de Correction atmosphérique Hyperspectrale d'Images de Senseurs Embarqués; [22]) and allows to estimate spectral signature at ground level according to simulated or measured spectral radiances by hyperspectral system.

The following hypotheses are retained : flat and homogeneous ground, surface temperature fixed to 293°K and atmosphere described by the standard atmospheric model (US Standard Atmosphere 1976) [21] with a integrated water vapour content set at 1.5 g.cm⁻².

The considered image acquisition system is the airborne hyperspectral instrument HYMAP [23] covering the spectral domain [0.4-2.5 µm] with a 128 spectral bands, a spectral resolution ranging from 15 to 20 nm and a spatial resolution around 4 meters at the height of 2000 meters.

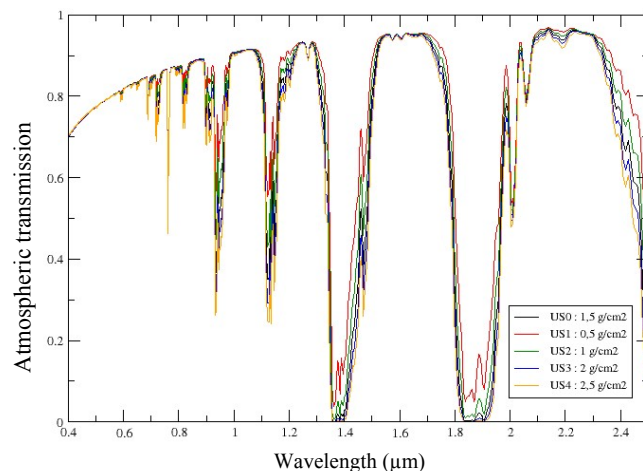
A nominal simulation case (called US0) is then defined according to the previous hypotheses and to measured spectral signatures chosen according to the following considerations (Table 6): a soil by spectral soil class and three SMC levels (dry, saturated and intermediary)

Table 6. Parameters of the nominal simulation case US0.

Hyperspectral system	HYMAP
Acquisition conditions	System altitude : 2 km Viewing angle : Nadir Hour : 11 TU
Climatic conditions	Atmospheric profile : US Standard Integrated vapour content : 1.5 g.cm ⁻²
Scene description	Surface temperature : 293 °K Measured spectral signature (one by soil spectral class) for three SMC levels varying from 0 % to 46 %

The impact of the atmospheric water vapour content on the SMC assessment methods is analyzed. The other four simulation cases (US1 to US4) correspond to the variation of the integrated vapour content from 0.5 g.cm⁻² to 2.5 g.cm⁻². This variation range has an impact on the absorption band width and the continuum of the atmospheric transmission (Figure 9).

Figure 9. Atmospheric transmission of the US standard profile for integrated vapor contents from 0.5 g.cm^{-2} to 2.5 g.cm^{-2} .

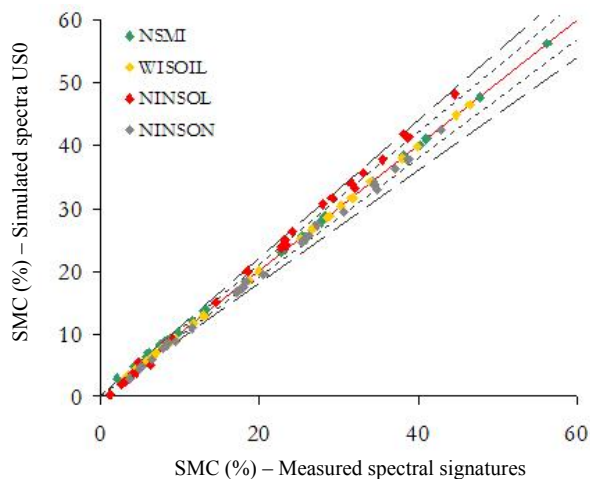


4.2.1 Impact of the Hyperspectral System and the Atmosphere

The local methods use specific wavelengths (see paragraph 3.1). They need to be adapted to the spectral bands of the retained hyperspectral system [6]. The deviation between the index wavelengths and the central wavelengths of the HYMAP spectral bands is, on average, lower than 3 nm.

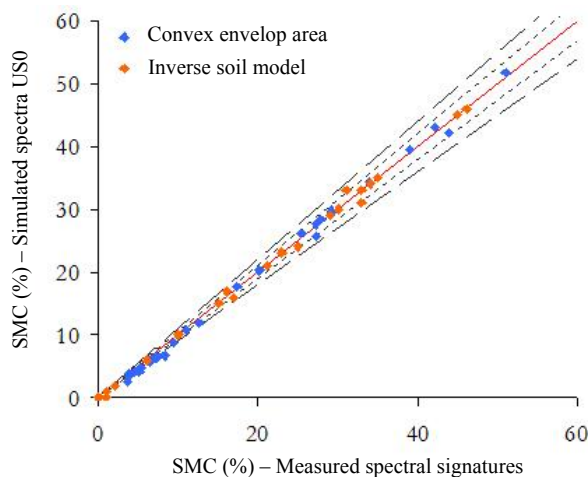
The atmosphere modelling and the instrumental specification integration have a low impact on the local method performances (Figure 10). The NSMI relative error is around 1 % for SMC higher than 15% and 10 % for SMC lower than 15 %. The WISOIL scatter plot is located close to the bisector (relative error in the order of 1.5 %). NINSOL tends to overestimate SMC. However it offers a relative error lesser than 10 % for SMC over 15 %. The NINSON relative error is about 5 %.

Figure 10. Local methods (NSMI, WISOIL, NINSOL, NINSON) – Representation of the SMC computed on the simulated spectra (nominal case US0) according to SMC assessed on the corresponding measured spectra (lines of small points on either side of centreline associated to the limit of a relative error of 5 % and the long-dashed lines representing the relative error equal to 10 %).



The global methods are not too sensitive to the introduction of the atmosphere and hyperspectral system bands (Figure 11). The relative error of the convex envelop area is 6 %. Its performance is comparable to NSMI according to the SMC levels. The ISER model is characterized by a relative error inferior to 10 % whatever the SMC value.

Figure 11. Global methods (convex envelop area, ISER model) – Representation of the SMC computed on the simulated spectra (nominal case US0) according to SMC assessed on the corresponding measured spectra (lines of small points on either side of centreline associated to the limit of a relative error of 5 % and the long-dashed lines representing the relative error equal to 10 %).

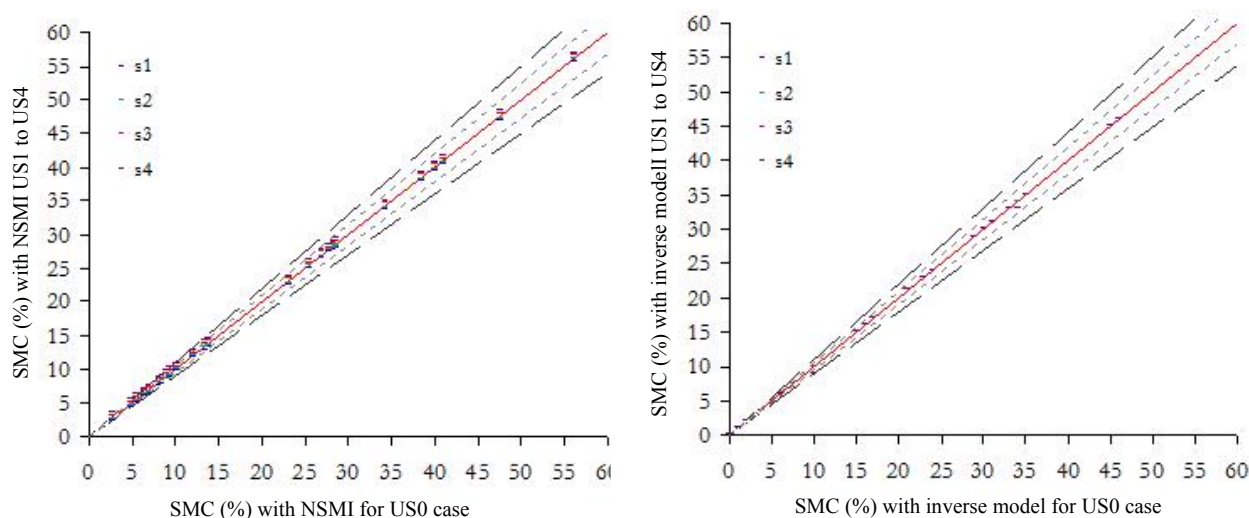


The overall SMC assessment methods are compared with respect to RMSE, assessed owing to measured SMC (see paragraph 4.1). The highest value is related to NSMI (around 8 %) and the lowest error is obtained with the inverse model (around 3 %). The convex envelop area and WISOIL deliver similar performances (around 7 %) as NINSOL and NINSON (around 6.5 %). These results are consistent with the findings of the methods applied on reference data (see paragraph 4.1).

4.2.2 Impact of the Atmospheric Water Vapour Content Variation (Simulation Cases US1 to US4)

The NSMI relative errors are lower than 5 % for SMC higher than 15% and lower than 10 % for lower SMC values, regardless of the atmospheric water vapour content. For instance, a water vapour content increase from 1.5 g.cm^{-2} to 2.5 g.cm^{-2} (US0 to US4) leads to a 6 % increase in average error of the SMC assessment (Figure 12). NSMI, operating with the Hymap spectral bands based on central wavelengths at $1.8 \mu\text{m}$ and $2.1228 \mu\text{m}$, is impacted by the water vapour content variation owing to the wavelength at $1.8 \mu\text{m}$ (Table 3). The SMC values are overestimated according to the increase in water vapour content (US3 and US4) and underestimated when it decreases (US1 and US2).

Figure 12. NSMI (right) and inverse soil model (left) results – Representation of assessed SMC for US1 to US4 cases according to the assessed SMC for the nominal case (US0). The short and long dashed lines represent respectively the limits of the relative error of 5 % and 10 %.



The variation of the water vapour absorption bandwidth has a low influence on WISOIL, NINSON and NINSOL owing to their operated wavelengths (Equations (4) and (5)). The average error on the SMC assessment is stable regardless of the simulation case (less than or equal to 1%).

The assessed SMC with the convex envelop area leads to relative error lower than 5 % for SMC values higher than 15 %. In this case, the increase of the water vapour content results in a significantly underestimation of the SMC value (if the water content increases from 1.5 g.cm^{-2} (US0) to 2.5 g.cm^{-2} (US4), the mean relative error increase of 16 %) and the water vapour content decrease leads to a SMC value overestimation (from 1.5 g.cm^{-2} (US0) to 0.5 g.cm^{-2} (US1), the average relative error increases

of 5 %). For SMC lower than 15%, the value are largely overestimated. The overestimation of the atmospheric water vapour content has an important impact for this method.

The ISER model is not influenced by changes in atmospheric water vapour content (Figure 12). The average relative error of SMC assessment is altered of 0.15% from US1 to US4.

To conclude, the least robust methods of SMC estimation to the atmospheric water content variation are NSMI and the convex envelop. WISOIL, NINSOL, NINSON and the ISER model are the less sensitive to the variation of this atmospheric parameter.

5 Conclusions

New global and local SMC estimation methods based on hyperspectral data of the reflective spectral domain [0.4-2.5 μm] are presented. These methods are validated on experimental and simulated data and are compared to existing methods in the literature.

The specification of SMC assessment criteria is lead owing to existing reference data measured in laboratory. Correlation matrixes are used to defined local methods based on spectral indexes which are compared to the spectral indexes in the literature (NSMI [6], WISOIL [2]). The proposed global methods include an improvement of the convex envelop model proposed by Whiting [7] and the inverse soil spectral model based on the semi-empirical soil spectral model proposed by [17]. This last one aims to estimating the SMC assuming that the soil spectral class (class related to the spectral behavior of the dry soil) is a priori known. All these methods are applied on a reference dataset in order to evaluate their performances.

The study based on the simulation of the realistic case (called nominal) corresponding to the modeling of the HyMap spectral bands and acquisition conditions and the atmosphere introduction leads to the definition of the most appropriate methods for estimating SMC. The errors are then lesser than 10 % and the most efficient methods are NINSOL and NINSON (RMSE of 6.5%) and the inverse soil spectral model (RMSE of 3%).

The sensitivity study in relation to the integrated atmospheric water vapor content has yielded the following results:

- Whatever the selected method and error, the most important impact is obtained for SMC lower than 15 %;
- NSMI and convex envelop area are lesser robust than the other methods;
- WISOIL, NINSOL and NINSON are slightly affected by the variation of atmospheric water vapor content;
- The inverse soil spectral model has the best performance.

In order to facilitate the effective application of the inverse soil spectral model, the first future works will be devoted to integrate soil class related to chemical analysis. It is necessary to first plan the introduction of this kind of soil class in the direct model. Finally, these methods will be tested and compared on real remote data acquired on a bare soil landscape in order to define rules for their use according to their robustness. The future works are expected to analyze the impact of sparse vegetation and adapt the methods for those items.

Acknowledgments

This study was funded by the PRF ENVIRO program (internal federative project lead at ONERA).

Author Contributions

All authors contributed to the work presented in this paper.

Conflicts of Interest

“The authors declare no conflict of interest”.

References and Notes

1. Vauclin, M. L'humidité des sols en hydrologie : intérêt et limites de la télédétection. Hydrological Applications of Remote Sensing and Remote Data Transmission, *Proceedings of the Hamburg Symposium* **1983**, IAHS 145.
2. Bryant, R.; Thoma, D.; Moran, S.; Holifield, C.; Goodrich, D.; Keefer, T.; Paige, G.; Williams, D.; Skirvin, S. Evaluation of Hyperspectral, Infrared Temperature and Radar Measurements for Monitoring Surface Soil Moisture. *Proceedings of the First Interagency Conference on Research in the Watersheds* **2003**, 27-30 October, Benson, Arizona, pp. 528-533.
3. Chabrillat, S.; Eisele, Guillaso, Rogäß, Ben-Dor, Kaufmann, H.; HYSOMA: An easy-to-use software interface for soil mapping applications of hyperspectral imagery, *Proceeding of: 7th EARSeL SIG Imaging Spectroscopy Workshop*, **2011**, Edinburgh, Scotland, UK, 11-13 April, Volume: 7pp.
4. Agenzia Spaziale Italiana; The PRISMA mission, *Document DC-OST-2009-124*, **2009**, Nota Informativa 04/04/09, pp.1-6.
5. EnMAP. Available online: <http://www.enmap.org/> (accessed on 27 03 2014).
6. Haubrock, S.; Chabrillat, S.; Lemmnitz, C.; Kaufmann, H. Surface soil moisture quantification models from reflectance data under field conditions. *International Journal of Remote Sensing* **2008**, Vol. 29, 1, pp. 3-29.
7. Whiting, M.L.; Li, L.; Ustin, S.L. Predicting water content using Gaussian model on soil spectra. *Remote Sensing of Environment* **2003**, vol. 89, pp. 535-552.
8. Angström, A. The albedo of various surfaces of ground. *Geografiska Annali* **1925**, 7, pp. 323-327.
9. Bach, H.; Mauser, W.; Modelling and model verification of the spectral reflectance of soils under varying moisture conditions. *Proc. IGARSS'94 Symposium* **1994**, Pasadena, vol. 4, pp. 2354-2356.
10. Liu, W.; Baret, F.; Gu, X.F.; Tong, Q.; Zheng, L.; Zhang, B. Relating soil surface moisture to reflectance. *Remote Sensing of Environment* **2002**, vol. 81, pp. 238-246.
11. Liu, W.; Baret, F.; Gu, X.; Tong, Q.; Zheng, L.; Zhang, B. Evaluation of methods for soil surface moisture estimation from reflectance data. *International Journal of Remote Sensing* **2003**, 24, pp. 2069-2083.

12. Khanna, S.; Palacios-Orueta, A.; Whiting, M.L.; Ustin, S.L.; Riaño, D.; Litago, J. Development of Angle Indexes for Soil Moisture Estimation, Dry Matter Detection and Land-cover Discrimination. *Remote Sensing of Environment* **2007**, *109*, pp. 154-165.
13. Lobell, D.; Asner, G. Moisture Effects on Soil Reflectance. *Soil Sciences American Journal* **2002**, *66*, pp. 722-727.
14. Ben-Dor, E.; Patkin, K.; Banin, A.; Karnieli, A. Mapping of several soil properties using DAIS-7915 hyperspectral scanner data – a case study over clayey soils in Israel. *International Journal of Remote Sensing* **2002**, Vol. 23, 6, 1043-1062.
15. Brocca, L.; Morbidelli, R.; Melone, F.; Moramarco, T. Soil Moisture spatial variability in experimental areas of central Italy. *Journal of Hydrology* **2007**, *333*, pp. 356-373
16. Sanchez, F. Soil Moisture Estimation by Hyperspectral Remote Sensing in the Doode Bemde area in the valley of the Dijle River, Flanders, Belgium. *Master dissertation in partial fulfilment of the requirements for the Degree of Master Science in Physical Land Resources* **2003**, Universiteit Brussel Belgium.
17. Lesaignoux, A.; Fabre, S.; Briottet, X. Influence of soil moisture content on spectral reflectance of bare soils in the 0.4–14 μm domain, *International Journal of Remote Sensing*, **2013**, *34*:7, pp. 2268-2285.
18. Munsell Soil Color Chart - 2009 Edition (Information available on line : <http://cspoutdoors.com/musococh20ed.html>)
19. Whiting, L.M.; Li, L.; Ustin, S.L. Predicting water content using Gaussian model on soil spectra, *Remote Sensing of Environment*, **2004**, vol. 89, pp. 535-552.
20. Berk, A.; Bernstein, L.S.; Anderson, G.P.; Acharya, P.K.; Robertson, D.C.; Chetwynd, J.H.; Adler-Golden, S.M.; MODTRAN cloud and multiple scattering upgrades with application to AVIRIS, *Remote Sensing of Environment*, **1998**, vol. 65, 367-375.
21. Berk, A.; Anderson, G.P.; Acharya, P.K.; Chetwynd, J.H.; Bernstein, L.S.; Shettle, E.P.; Matthew, M.W.; Adler-Golden, S.M.; *MODTRAN4 USER'S MANUAL*, **1999**, Air Force Research Laboratory.
22. Miesch, C.; Poutier, L.; Achard, V.; Briottet, X.; Lenot, X.; Boucher, Y. ; Direct and inverse radiative transfer solutions for visible and near infrared hyperspectral imagery, *IEEE Transactions on Geosciences and Remote Sensing*, **2005**, vol. 43(7).
23. Cocks, T.; Jenssen, R.; Stewart, A.; Wilson, I.; Shields, T.; The HyMap Airborne Hyperspectral Sensor: The System, Calibration and Performance, *Proceedings 1st EARSeL Workshop on Imaging Spectroscopy*, **1998**, Zurich, p. 37-43, 6-8 October.